Reshaping the amyloid buildup curve in Alzheimer's disease? – Partial volume effect correction of longitudinal amyloid PET data

Michael Rullmann*[1], Anke McLeod[1], Michel J. Grothe[2], Osama Sabri[1], Henryk Barthel[1] and The Alzheimer Disease Neuroimaging Initiative[†]

[1] Department of Nuclear Medicine, University of Leipzig, Germany

[2] German Center for Neurodegenerative Diseases (DZNE) - Rostock/Greifswald, Rostock, Germany.

[†] Data used in preparation of this article were obtained from the Alzheimer's Disease Neuroimaging Initiative (ADNI) database (adni.loni.usc.edu). As such, the investigators within the ADNI contributed to the design and implementation of ADNI and/or provided data but did not participate in analysis or writing of this report. A complete listing of ADNI investigators can be found at: http://adni.loni.usc.edu/wp-content/uploads/how_to_apply/ADNI_Acknowledgement_List.pdf

* Corresponding Author:
Dr. Michael Rullmann
Department of Nuclear Medicine
University of Leipzig
Liebigstrasse 18
D-04103 Leipzig
Germany
rullmann@medizin.uni-leipzig.de

Short running title: PVEC of longitudinal amyloid PET

Word count of whole manuscript: 3916

ABSTRACT

It was hypothesized that the brain β-amyloid buildup curve plateaus at an early symptomatic Alzheimer´s disease (AD) stage. Atrophy-related partial volume effects (PVEs) degrade signal in hot-spot imaging techniques, such as amyloid positron emission tomography (PET). This longitudinal analysis of amyloid-sensitive PET data investigated the shape of the β-amyloid curve in AD applying PVE correction (PVEC).

We analyzed baseline and 2-year follow-up data of 216 symptomatic individuals on the AD continuum (positive amyloid status) enrolled in Alzheimer's Disease Neuroimaging Initiative (17 AD dementia, 199 mild cognitive impairment), including 18F-florbetapir PET, magnetic resonance imaging and mini mental state examination (MMSE) scores. For PVEC, the modified Müller-Gärtner method was performed.

Compared to non-PVE-corrected data, PVE-corrected data yielded significantly higher regional and composite standardized uptake value ratio (SUVR) changes over time (P=0.0002 for composite SUVRs). Longitudinal SUVR changes in relation to MMSE decreases showed a significantly higher slope of the regression line in the PVE-corrected as compared to the non-PVE-corrected PET data (F=7.1, P=0.008).

These PVEC results indicate that the β-amyloid buildup curve does not plateau at an early symptomatic disease stage. A further evaluation of the impact of PVEC on the in-vivo characterization of time-dependent AD pathology, including the reliable assessment and comparison of other amyloid tracers, is warranted.

Keywords: positron emission tomography, amyloid, longitudinal, partial volume effect correction

LIST OF ABBREVIATIONS

AD - Alzheimer's disease

ADNI - Alzheimer's Disease Neuroimaging Initiative

MCI - mild cognitive impairment

l/r - left and right

MMSE - mini mental state examination

MR - magnetic resonance

PET - positron emission tomography

PVE – partial volume effect

PVEC - partial volume effect correction

SUVR - standardized uptake value ratio

INTRODUCTION

The amyloid cascade theory of Alzheimer's disease (AD) (*1*) assumes that brain β-amyloid aggregation is an early, possibly causative event, which triggers neurodegenerative processes, such as tau accumulation, synaptic dysfunction and atrophy, leading to the distinct dementia phenotype. Currently, it is hypothesized that the cerebral β-amyloid buildup already plateaus at an early disease stage at which tau accumulation and neurodegeneration still accelerate and first cognitive symptoms occur (*2*). Postmortem studies have failed to demonstrate a stringent relationship between severity of cognitive impairment and density of amyloid plaques (*3*). Evidence for the β-amyloid buildup curve in AD reaching a plateau at an early symptomatic disease stage was provided by cross-sectional (*4*) and longitudinal (*5,6*) analysis of β-amyloid positron emission tomography (PET) data. However, these studies did not account for atrophy-related partial volume effects (PVEs), which have recently been identified as a major signal confound in hot-spot imaging techniques, such as β-amyloid PET (*7*). PVE correction (PVEC) compensates for these resolution-induced inaccuracies improving quantitative accuracy (*8-11*) and discrimination between patients with cognitive impairment and healthy controls (*10-13*). Assessing cognition, disease stage and longitudinal 18F-florbetapir PET imaging we investigated whether a plateau-shaped β-amyloid build-up curve also holds when applying appropriate PVEC methods to the PET data.

MATERIALS AND METHODS

Based on data from the Alzheimer's Disease Neuroimaging Initiative (ADNI) database, we extracted all available 18F-florbetapir amyloid PET datasets from participants with (1) AD dementia or mild cognitive impairment (MCI) diagnosis, (2) at least two PET visits, (3) corresponding magnetic resonance (MR) scans for each PET scan within ± 50 days and (4) corresponding mini mental state examination (MMSE) (14) scores for each visit. These criteria were fulfilled by 312 patients (22 AD, 290 MCI). If available, we also extracted the corresponding cerebrospinal fluid levels of β-amyloid (Aβ$_{1-42}$) from the ADNI database. The study was approved by ADNI and written informed consent was obtained by ADNI from all subjects.

PVEC was performed as previously described (10). In short, the MR data were resliced to 1 mm isotropic voxel size. PVElab (15), which requires full-width at half maximum specifications of the applied PET scanner, was used to correct the PET data PVEs. This included coregistration of MR and PET data, reslicing of PET data to MR space, segmentation of MR data, Montreal Neurological Institute-based labeling and voxelwise PVEC using the modified Müller-Gärtner approach (16,17). PVElab automatically computed the mean activity concentrations for the following atlas regions: hippocampus left and right (l/r), anterior and posterior cingulate cortex, deep gray matter, occipital cortex, frontal cortex (l/r), temporal cortex (l/r), parietal cortex (l/r), Brodmann area 9 (l/r), cerebellar cortex, white matter and cerebrospinal fluid. Regional standardized uptake value ratios (SUVRs) were computed using the cerebellar cortex as reference region (18). In addition, we calculated a composite SUVR of the volume-weighted means from frontal cortex, parietal cortex, occipital cortex, temporal cortex, anterior and posterior cingulate cortex (19). We validated the applied PVEC pipeline using an alternative PVEC called region-based voxel-wise correction method (8).

In order to limit our analysis to cases on the AD continuum we applied a threshold of 1.1 for the uncorrected composite SUVR to include only amyloid-positive subjects (20) (N = 64 excluded). We excluded data lacking the transaxial and axial full-width at half maximum specifications, as outlined by the National Electrical Manufacturers Association, for the respective PET scanners (required for correct PVEC, N = 18 excluded). Further, PVEC outliers (PVE-corrected composite SUVR < mean-2sd or > mean+2sd) were excluded (N = 14 excluded). The final sample of the presented analysis included data of 216 participants comprising 17 patients with AD dementia and 199 subjects with MCI.

Statistical analyses were performed in Matlab. We applied paired t-tests to evaluate difference scores in SUVR change over time between PET data with and without PVEC. Regression analysis of composite SUVRs and their corresponding MMSE scores as well as cerebrospinal fluid biomarker levels included a comparison of beta coefficients between the PET data with and without PVEC. The relationship between SUVR changes over time and baseline MMSE scores was evaluated using a linear regression model (dependent variable: extracted SUVR changes; independent variable: baseline MMSE scores), where the slope coefficient significance was tested using the one-sided t test, representing the biologically reasonable association. For all tests, significance was assumed at the $P < 0.05$ level

Data availability

Data used in the preparation of this article were obtained from the ADNI database. For up-to-date information, see http://www.adni-info.org.

RESULTS

The AD patients and MCI individuals did not differ regarding longitudinal imaging time points and demographic data, apart from age (p=0.03) and the MMSE scores at baseline (p<0.0001, Table 1).

Figure 1 shows the baseline and 2-year follow-up MR as well as the gray matter-masked amyloid PET data with and without PVEC together with illustrations of the respective relative SUVR changes over time in a paradigmatic AD patient who deteriorated in MMSE scores from 25 to 21. In this case, SUVR increases were more pronounced in the PVE-corrected as compared to uncorrected PET data.

Overall, the PVE-corrected PET data revealed significantly higher SUVR changes over time as compared to the non-corrected PET data in the composite region (P = 0.0002), as well as in left hippocampus (P = 0.03), anterior cingulate cortex (P = 0.001), occipital cortex (P = 0.02), bilateral frontal cortex (left, P = 0.00004; right, P = 0.000002), bilateral temporal cortex (left, P = 0.0005; right, P = 0.0008), bilateral parietal cortex (left, P = 0.0007; right, P = 0.002), and bilateral Brodmann area 9 (left, P = 0.0003; right, P = 0.00002)(Table 2, Supplement Figure 1). Thereby, the Cohen's d effect sizes seem to be higher in AD patients compared to MCI participants, e.g. in the composite region 0.57 and 0.19, respectively (Supplement Table 1).

The linear regressions between time-dependent composite SUVRs and time-dependent MMSE scores with and without PVEC are shown in Figure 2. Here, the slope for the PVE-corrected PET data was significantly steeper when compared to the uncorrected data (F = 7.1, P = 0.008). Significant steeper slopes were also found for PVE-corrected PET data in the linear regressions between baseline composite SUVRs and cerebrospinal fluid levels of β-amyloid (F = 16.2, P = 7.7×10^{-5}).

Further, only PVE-corrected composite SUVR changes correlated significantly, albeit weakly, with baseline MMSE scores (PVE-corrected: r = -0.11, P = 0.049, non-corrected: r = -0.07, P = 0.16).

All findings were reproduced using the region-based voxel-wise PVEC (see Supplement) (*8*),(*21*)–(*24*).

DISCUSSION

In the present report, the effect of PVEC on longitudinal 18F-florbetapir amyloid PET data and its association with cognitive impairment was evaluated. Over time, PVE-corrected PET data, compared to uncorrected data, showed significantly higher regional and composite SUVR changes. Further, with advancing cognitive impairment, a longitudinal β-amyloid buildup dynamic can be visualized by applying PVEC.

In agreement, several papers have consistently found that PVE-uncorrected β-amyloid PET data leads to quantitative underestimation (*6,9,10*). In principal, Gonzalez-Escamilla et al. also supported the notion of a PVEC-associated SUVR increase, but only in high-amyloid cases.

No consensus on whether PVEC is imperative has been reached yet. Its implementation in AD research has been recommended as it improves clinical classification performance (*25*) and optimizes the longitudinal measure of β-amyloid (*26*). However, Schwarz et al., for example, illustrated that imprecision in β-amyloid load measurements due to PET-MR rigid registration is larger when applying PVEC (*27*).

In a 11C-Pittsburgh compound B PET study, Villemagne et al. reported on small, significant increases in tracer uptake over a 20-month period for MCI and AD groups after applying PVEC (*6*). Brendel et al. substantiated the PVEC-associated improved discriminatory power effect in a large scale, longitudinal 18F-florbetapir PET study of 962 individuals.

Given that the amyloid deposition potentially follows a sigmoid trajectory as a function of time (*2*), our description of a continuous increase in early symptomatic AD cases challenges the concept of β-amyloid reaching a plateau at a much earlier stage of the disease. Notably, Villemagne et al. (2011) performed the same analysis on the data with and without PVEC (modified Müller-Gärtner) and stated that the results did not significantly differ (*6*). This discrepancy to our present findings may relate to the employment of different tracers and their different behavior in white matter uptake (*28*).

Assessing cognition, it is currently understood that β-amyloid deposition is associated with cognitive dysfunction in the early stages of decline but essentially decoupled from AD progression at later disease stages (*29*),(*30*). In fact, at moderate and later stages of disease, advancing cognitive impairment appears to be more closely linked to glucose hypometabolism (*31*) and tau

pathophysiology (*32*). Yet, by utilizing longitudinal 18F-florbetapir PET data and applying the modified Müller-Gärtner PVEC method, we found that cortical amyloid load continued to increase in parallel with cognitive impairment in the symptomatic stages of AD. The slope for the association between longitudinal tracer uptake and declining cognitive performance was significantly steeper for PVE-corrected PET data compared to uncorrected data. Thus, when using more appropriate methods for amyloid-PET tracer quantification there is little evidence to suggest that the β-amyloid buildup does plateau at an early disease stage. Further, only after PVEC, we found that composite SUVR changes correlated negatively with baseline MMSE scores. However, our findings are somewhat at odds with previous results that reported on an inverse, positive relationship; that is, greater increase in tracer uptake was reported in clinically milder AD patients (*6*) as opposed to those at later stages of the disease.

Analyzing cortical vs subcortical 18F-florbetapir PET tracer uptake, Chou et al. described a downward spreading pattern of β-amyloid with initial accumulation in the neocortex being followed by the affection of subcortical structures. Hereby, subcortical involvement at later stages of the disease, compared to cortical-only involvement (*33*), implied worse cognitive function and a steeper decline during follow-up (*34*).

However, no PVEC was performed in this study as opposed to further research directed at characterizing regionally more comprehensive in-vivo staging schemes of progressive cerebral amyloid deposition (*35*).

A limitation of our analysis is that only one particular PVEC method (modified Müller-Gärtner) was performed. This 3-compartmental technique explicitly corrects for both CSF spill-out and spill-in of high intensity WM signal and is thus a much more appropriate approach for correcting typical PVEs in amyloid-PET data than the 2-comparmental alternative represented by the widely used "Meltzer" method (*36*),(*37*). However, several other PVEC techniques for amyloid imaging have been described (*38*), but clinically a consensus on the use, and exact implementation, of PVEC for amyloid-PET is yet to be reached.

CONCLUSION

In conclusion, the reliable interpretation of longitudinal amyloid deposition and its relationship to the clinical course in early symptomatic stages of AD has been investigated. Our analysis indicates that PVEC should be used to improve quantification accuracy of longitudinal β-amyloid PET data to allow visualization of the gradual β-amyloid buildup dynamic during cognitive decline, which does not appear to plateau at early symptomatic stages according to our data. Our results imply that a further evaluation of the impact of PVEC on the in-vivo characterization of time-dependent amyloid pathology in AD, including the reliable assessment and comparison of other amyloid tracers and PVEC methods, is warranted.

ACKNOWLEDGEMENTS

KEY POINTS

Question: Does the shape of the brain β-amyloid buildup curve in Alzheimer´s disease changes by applying partial volume effect correction (PVEC) on longitudinal amyloid PET data?

Pertinent Finding: In a large sample of subjects with Alzheimer´s disease or mild cognitive impairment (N = 216 from ADNI), the application of PVEC on longitudinal amyloid PET data changes the amyloid buildup curve from a plateau to an increase.

Implications for Patient Care: This new knowledge motivates to regularly employ PVEC in the future in analyzing longitudinal amyloid PET data for disease progression/therapy monitoring.

COMPETING INTERESTS

The authors report no competing interests.

REFERENCES

1. Hardy JA, Higgins GA. Alzheimer's disease: the amyloid cascade hypothesis. *Science*. 1992;256:184-185.
2. Jack CR, Knopman DS, Jagust WJ, et al. Hypothetical model of dynamic biomarkers of the Alzheimer's pathological cascade. *Lancet Neurol*. 2010;9:119-128.
3. Prohovnik I, Perl DP, Davis KL, Libow L, Lesser G, Haroutunian V. Dissociation of neuropathology from severity of dementia in late-onset Alzheimer disease. *Neurology*. 2006;66:49-55.
4. Doraiswamy PM, Sperling RA, Johnson K, et al. Florbetapir F 18 amyloid PET and 36-month cognitive decline: a prospective multicenter study. *Mol Psychiatry*. 2014;19:1044-1051.
5. Villemagne VL, Burnham S, Bourgeat P, et al. Amyloid β deposition, neurodegeneration, and cognitive decline in sporadic Alzheimer's disease: A prospective cohort study. *Lancet Neurol*. 2013;12:357-367.
6. Villemagne VL, Pike KE, Chételat G, et al. Longitudinal assessment of Aβ and cognition in aging and Alzheimer disease. *Ann Neurol*. 2011;69:181-192.
7. Matsubara K, Ibaraki M, Shimada H, et al. Impact of spillover from white matter by partial volume effect on quantification of amyloid deposition with 11CPiB PET. *Neuroimage*. 2016;143:316-324.
8. Thomas BA, Erlandsson K, Modat M, et al. The importance of appropriate partial volume correction for PET quantification in Alzheimer's disease. *Eur J Nucl Med Mol Imaging*. 2011;38:1104-1119.
9. Su Y, Blazey TM, Snyder AZ, et al. Partial volume correction in quantitative amyloid imaging. *Neuroimage*. 2015;107:55-64.
10. Rullmann M, Dukart J, Hoffmann K-T, et al. Partial-Volume Effect Correction Improves Quantitative Analysis of 18F-Florbetaben β-Amyloid PET Scans. *J Nucl Med*. 2016;57:198-203.
11. Gonzalez-Escamilla G, Lange C, Teipel S, Buchert R, Grothe MJ. PETPVE12: an SPM toolbox for Partial Volume Effects correction in brain PET - Application to amyloid imaging with AV45-PET. *Neuroimage*. 2017;147:669-677.
12. Mikhno A, Devanand D, Pelton G, et al. Voxel-based analysis of 11C-PIB scans for diagnosing Alzheimer's disease. *J Nucl Med*. 2008;49:1262-1269.
13. Brendel M, Högenauer M, Delker A, et al. Improved longitudinal (18)F-AV45 amyloid PET by white matter reference and VOI-based partial volume effect correction. *Neuroimage*. 2015;108:450-459.
14. Folstein MF, Folstein SE, McHugh PR. "Mini-mental state". A practical method for grading the cognitive state of patients for the clinician. *J Psychiatr Res*. 1975;12:189-198.
15. Quarantelli M, Berkouk K, Prinster A, et al. Integrated software for the analysis of brain PET/SPECT studies with partial-volume-effect correction. *J Nucl Med*. 2004;45:192-201.
16. Müller-Gärtner HW, Links JM, Prince JL, et al. Measurement of radiotracer concentration in brain gray matter using positron emission tomography: MRI-based correction for partial volume effects. *J Cereb Blood Flow Metab*. 1992;12:571-583.
17. Rousset OG, Ma Y, Evans AC. Correction for partial volume effects in PET: Principle and validation. *J Nucl Med*. 1998;39:904-911.
18. Catafau AM, Bullich S, Seibyl JP, et al. Cerebellar Amyloid-β Plaques: How Frequent Are They, and Do They Influence 18F-Florbetaben SUV Ratios? *J Nucl Med*. 2016;57:1740-1745.

19. Barthel H, Gertz H-J, Dresel S, et al. Cerebral amyloid-β PET with florbetaben (18F) in patients with Alzheimer's disease and healthy controls: A multicentre phase 2 diagnostic study. *Lancet Neurol*. 2011;10:424-435.

20. Johnson KA, Sperling RA, Gidicsin CM, et al. Florbetapir (F18-AV-45) PET to assess amyloid burden in Alzheimer's disease dementia, mild cognitive impairment, and normal aging. *Alzheimers Dement*. 2013;9:S72-83.

21. Hammers A, Allom R, Koepp MJ, et al. Three-dimensional maximum probability atlas of the human brain, with particular reference to the temporal lobe. *Hum Brain Mapp*. 2003;19:224-247.

22. Gousias IS, Rueckert D, Heckemann RA, et al. Automatic segmentation of brain MRIs of 2-year-olds into 83 regions of interest. *Neuroimage*. 2008;40:672-684.

23. Faillenot I, Heckemann RA, Frot M, Hammers A. Macroanatomy and 3D probabilistic atlas of the human insula. *Neuroimage*. 2017;150:88-98.

24. Thomas BA, Cuplov V, Bousse A, et al. PETPVC: a toolbox for performing partial volume correction techniques in positron emission tomography. *Phys Med Biol*. 2016;61:7975-7993.

25. Yang J, Hu C, Guo N, et al. Partial volume correction for PET quantification and its impact on brain network in Alzheimer's disease. *Sci Rep*. 2017;7:13035.

26. Schwarz CG, Senjem ML, Gunter JL, et al. Optimizing PiB-PET SUVR change-over-time measurement by a large-scale analysis of longitudinal reliability, plausibility, separability, and correlation with MMSE. *Neuroimage*. 2017;144:113-127.

27. Schwarz CG, Jones DT, Gunter JL, et al. Contributions of imprecision in PET-MRI rigid registration to imprecision in amyloid PET SUVR measurements. *Hum Brain Mapp*. 2017;38:3323-3336.

28. Su Y, Flores S, Wang G, et al. Comparison of Pittsburgh compound B and florbetapir in cross-sectional and longitudinal studies. *Alzheimers Dement (Amst)*. 2019;11:180-190.

29. Jack CR, Wiste HJ, Vemuri P, et al. Brain beta-amyloid measures and magnetic resonance imaging atrophy both predict time-to-progression from mild cognitive impairment to Alzheimer's disease. *Brain*. 2010;133:3336-3348.

30. Rowe CC, Ng S, Ackermann U, et al. Imaging beta-amyloid burden in aging and dementia. *Neurology*. 2007;68:1718-1725.

31. Landau SM, Mintun MA, Joshi AD, et al. Amyloid deposition, hypometabolism, and longitudinal cognitive decline. *Ann Neurol*. 2012;72:578-586.

32. Aschenbrenner AJ, Gordon BA, Benzinger TLS, Morris JC, Hassenstab JJ. Influence of tau PET, amyloid PET, and hippocampal volume on cognition in Alzheimer disease. *Neurology*. 2018;91:e859-e866.

33. Hanseeuw BJ, Betensky RA, Mormino EC, et al. PET staging of amyloidosis using striatum. *Alzheimers Dement*. 2018;14:1281-1292.

34. Cho SH, Shin J-H, Jang H, et al. Amyloid involvement in subcortical regions predicts cognitive decline. *Eur J Nucl Med Mol Imaging*. 2018;45:2368-2376.

35. Grothe MJ, Barthel H, Sepulcre J, Dyrba M, Sabri O, Teipel SJ. In vivo staging of regional amyloid deposition. *Neurology*. 2017;89:2031-2038.

36. Butters MA, Klunk WE, Mathis CA, et al. Imaging Alzheimer pathology in late-life depression with PET and Pittsburgh Compound-B. *Alzheimer Dis Assoc Disord*. 2008;22:261-268.

37. Lowe VJ, Kemp BJ, Jack CR, et al. Comparison of 18F-FDG and PiB PET in cognitive impairment. *J Nucl Med*. 2009;50:878-886.

38. Shidahara M, Thomas BA, Okamura N, et al. A comparison of five partial volume correction methods for Tau and Amyloid PET imaging with (18)FTHK5351 and (11)CPIB. *Ann Nucl Med*. 2017;31:563-569.
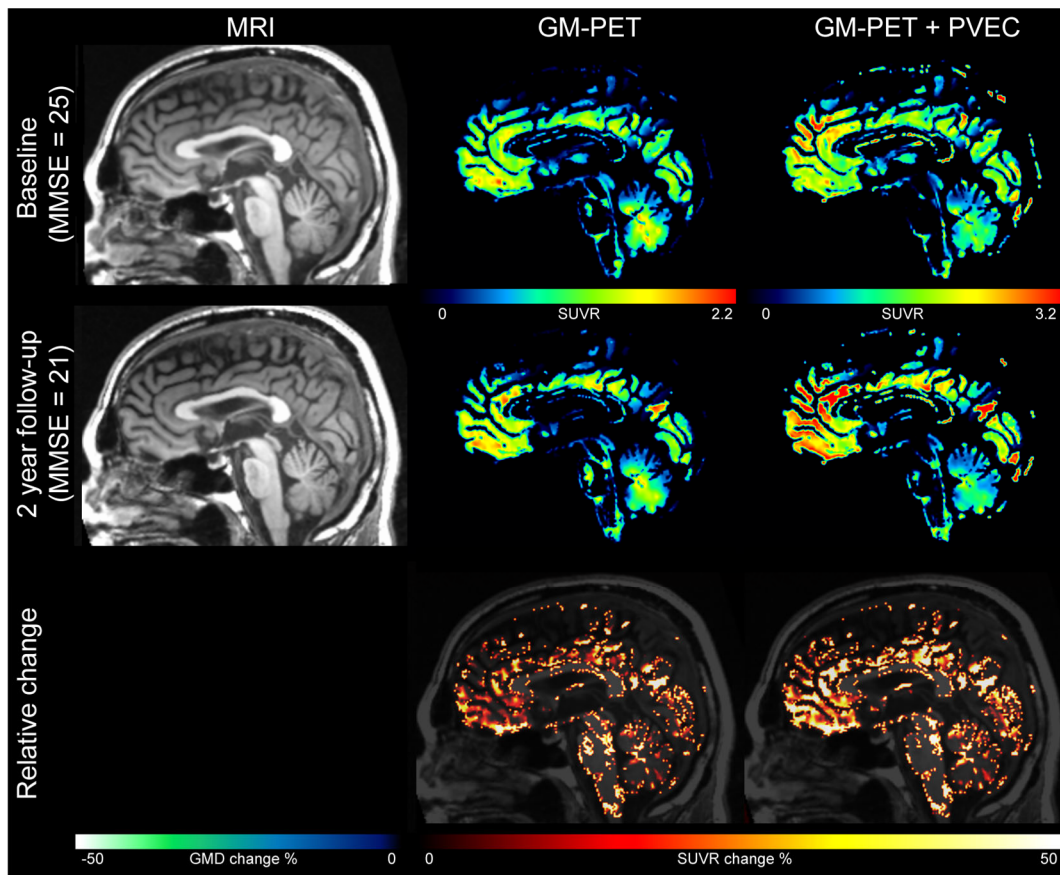
Figure 1: Example of amyloid PET/MR data with and without PVEC over time. Baseline (top row) and 2-year follow-up (middle row) MR (left column) and gray matter (GM)-masked 18F-florbetapir PET data without (middle column) and with (right column) partial volume effect correction (PVEC) of an Alzheimer's dementia patient. Relative standardized uptake value ratio (SUVR) increase over time (bottom row) was higher with vs. without PVEC. MMSE: Mini mental state examination.
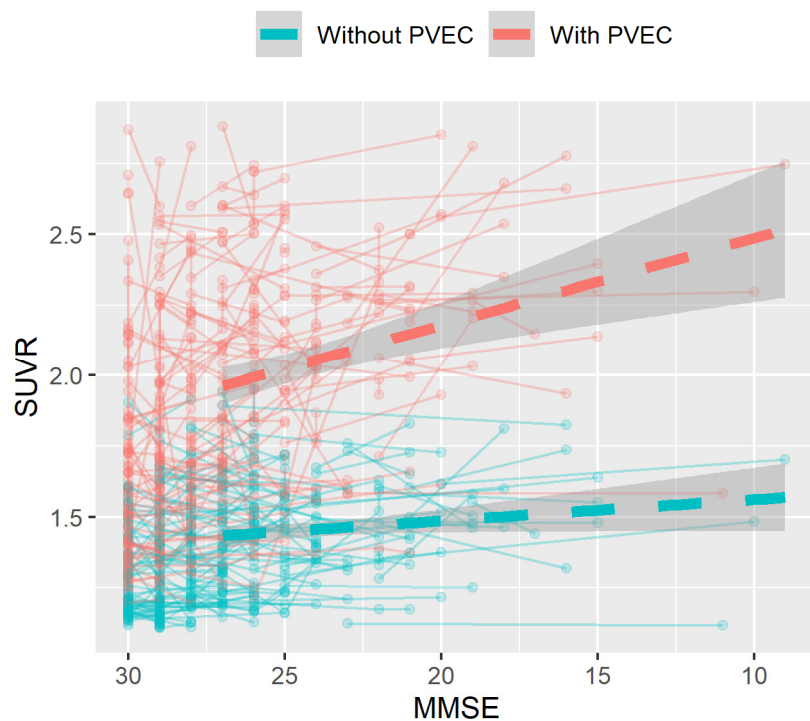
Figure 2: Effect of PVEC on correlation of MMSE and amyloid PET. Regression analysis of baseline-to-follow-up composite standardized uptake ratio values (SUVRs) vs. baseline-to-follow-up mini mental state examination (MMSE) scores for amyloid PET data with vs. without partial volume effect correction (PVEC). Significantly steeper slope in case of the PVE-corrected data ($F = 7.1$, $P = 0.008$). Only data with baseline MMSE scores < 28 were included in this analysis.

17

TABLES

Table 1: Demographics of the study cohort

	AD	MCI	P
N	17	199	-
One/two PET follow-ups	17/0	179/20	0.38[a]
Age at baseline [years]	76 ± 6	71 ± 8	0.03[b]
Gender (♀/♂)	8/9	84/115	0.8[a]
MMSE at baseline	22.4 ± 1.8	28 ± 1.8	$5.2*10^{-27}$[b]
Time range between PET and corresponding MR scan [days]	15 ± 12	14 ± 12	0.34[b]
Time range between PET assessments [years]	2.0 ± 0.1	2.1 ± 0.3	0.63[b]

AD: Alzheimer's dementia; MCI: mild cognitive impairment; MMSE: Mini mental state examination; [a]Fisher's exact test; [b]ANOVA

Table 2: Influence of partial volume effect correction (PVEC) on standardized uptake value ratio changes over time

Region	Without PVEC	With PVEC	P
Left frontal cortex	0.023 ± 0.14	0.067 ± 0.25	$4.4*10^{-5}$
Right frontal cortex	0.022 ± 0.13	0.071 ± 0.23	$1.6*10^{-6}$
Left temporal cortex	0.015 ± 0.11	0.058 ± 0.25	$5.4*10^{-4}$
Right temporal cortex	0.017 ± 0.12	0.061 ± 0.27	$7.5*10^{-4}$
Left parietal cortex	0.017 ± 0.15	0.070 ± 0.30	$6.7*10^{-4}$
Right parietal cortex	0.021 ± 0.14	0.074 ± 0.32	$1.7*10^{-3}$
Left hippocampus	0.007 ± 0.31	0.044 ± 0.50	0.027
Right hippocampus	-0.007 ± 0.28	0.013 ± 0.35	0.17
Left Brodmann area 9	0.033 ± 0.17	0.085 ± 0.34	$3.3*10^{-4}$
Right Brodmann area 9	0.030 ± 0.15	0.084 ± 0.30	$1.8*10^{-5}$
Anterior cingulate	0.018 ± 0.14	0.063 ± 0.28	$1.2*10^{-3}$
Occipital	0.009 ± 0.10	0.047 ± 0.27	0.023
Composite	0.017 ± 0.11	0.061 ± 0.22	$1.9*10^{-4}$

Reshaping the amyloid buildup curve in Alzheimer's disease? – Partial volume effect correction of longitudinal amyloid PET data

Michael Rullmann[1], Anke McLeod[1], Michel J. Grothe[2], Osama Sabri[1], Henryk Barthel[1] and The Alzheimer Disease Neuroimaging Initiative[†]

[1] Department of Nuclear Medicine, University of Leipzig, Germany

[2] German Center for Neurodegenerative Diseases (DZNE) - Rostock/Greifswald, Rostock, Germany.

SUPPLEMENT MATERIAL

MATERIALS AND METHODS

We validated the applied PVEC pipeline using an alternative PVEC called region-based voxel-wise (RBV) correction method (*1*).

For that purpose, we used the inverse of the spatial transformation to transfer the Hammers atlas (*2-4*) to the individual space. We then used the individual gray and white matter segmentation to mask the Hammers atlas. The masked atlas, PET data and FWHM parameter of the corresponding PET scanner were used as input to calculate RBV-PVEC images using the PETPVC toolbox (*5*).

RESULTS

Overall, the RBV-PVE-corrected PET data revealed significantly higher SUVR changes over time as compared to the non-corrected PET data in the composite region ($P = 4.1 \times 10^{-8}$), as well as the anterior cingulate cortex ($P = 9.8 \times 10^{-9}$), posterior cingulate cortex ($P = 1.7 \times 10^{-13}$), occipital cortex ($P = 6.4 \times 10^{-9}$), frontal cortex ($P = 1.7 \times 10^{-5}$), temporal cortex ($P = 5.6 \times 10^{-9}$), and parietal cortex ($P = 1.1 \times 10^{-6}$).

The slope of linear regressions between time-dependent composite SUVRs and time-dependent MMSE scores for the RBV-PVE-corrected PET data was significantly steeper when compared to the uncorrected data (F = 4.44, P = 0.035). While we observed significant correlations of both, RBV-PVE-corrected and uncorrected PET data with CSF levels of β-amyloid, there were no significant differences in slopes here.
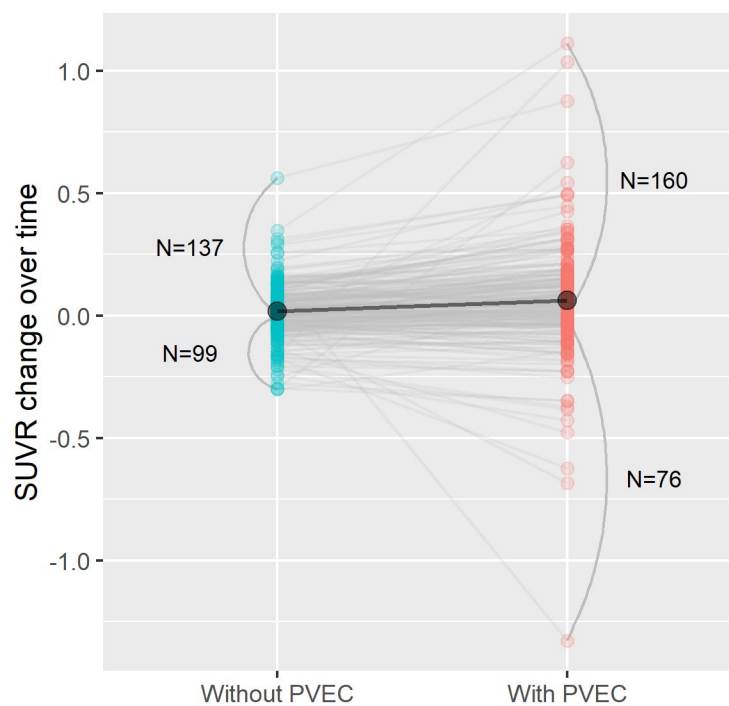
Further, only RBV-PVE-corrected composite SUVR changes correlated significantly with baseline MMSE scores (two-sided t test, RBV-PVE-corrected: r = -0.13, P = 0.02, non-corrected: r = -0.10, P = 0.06).

2

TABLES

Supplement Table 1: Influence of partial volume effect correction (PVEC) on standardized uptake value ratio changes over time separated for AD and MCI patients.

Region	AD				MCI			
	Without PVEC	With PVEC	P	Cohen's d	Without PVEC	With PVEC	P	Cohen's d
Left frontal cortex	-0.023 ± 0.20	0.024 ± 0.28	0.09	0.13	0.027 ± 0.14	0.070 ± 0.25	0.0001	0.17
Right frontal cortex	-0.019 ± 0.20	0.058 ± 0.24	0.03	0.33	0.025 ± 0.12	0.072 ± 0.23	1.1×10^{-5}	0.20
Left temporal cortex	0.027 ± 0.15	0.194 ± 0.41	0.05	0.42	0.014 ± 0.11	0.048 ± 0.23	0.004	0.15
Right temporal cortex	0.039 ± 0.17	0.213 ± 0.42	0.03	0.36	0.015 ± 0.11	0.049 ± 0.26	0.007	0.13
Left parietal cortex	-0.054 ± 0.26	0.058 ± 0.26	0.11	0.43	0.022 ± 0.14	0.071 ± 0.30	0.002	0.17
Right parietal cortex	-0.035 ± 0.21	0.098 ± 0.30	0.12	0.51	0.025 ± 0.13	0.072 ± 0.32	0.006	0.15
Left hippocampus	-0.129 ± 0.28	0.058 ± 0.16	0.06	0.85	0.002 ± 0.28	0.009 ± 0.36	0.61	0.02
Right hippocampus	-0.122 ± 0.43	-0.070 ± 0.54	0.12	0.05	0.017 ± 0.30	0.053 ± 0.50	0.045	0.06
Left Brodmann area 9	0.005 ± 0.21	0.028 ± 0.49	0.76	0.03	0.035 ± 0.16	0.090 ± 0.33	0.0002	0.15
Right Brodmann area 9	0.029 ± 0.22	0.081 ± 0.44	0.40	0.07	0.031 ± 0.15	0.084 ± 0.29	2.2×10^{-5}	0.16
Anterior cingulate	0.036 ± 0.17	0.199 ± 0.47	0.08	0.33	0.016 ± 0.13	0.052 ± 0.26	0.007	0.15
Occipital	0.010 ± 0.14	0.165 ± 0.28	0.04	0.67	0.009 ± 0.10	0.038 ± 0.26	0.09	0.13
Composite	-0.003 ± 0.16	0.121 ± 0.25	0.04	0.57	0.018 ± 0.11	0.057 ± 0.22	0.001	0.19

FIGURES

Supplement Figure 1: Effect of PVEC on SUVR changes over time. On average, the SUVR changes over time in the composite region increased after PVEC (P = 1.9×10^{-4}). The amount of participants presenting SUVR increase and decrease over time is annotated for PVE-corrected and uncorrected data beside the curved lines.

REFERENCES

1. Thomas BA, Erlandsson K, Modat M, et al. The importance of appropriate partial volume correction for PET quantification in Alzheimer's disease. *Eur J Nucl Med Mol Imaging*. 2011;38:1104-1119.
2. Hammers A, Allom R, Koepp MJ, et al. Three-dimensional maximum probability atlas of the human brain, with particular reference to the temporal lobe. *Hum Brain Mapp*. 2003;19:224-247.
3. Gousias IS, Rueckert D, Heckemann RA, et al. Automatic segmentation of brain MRIs of 2-year-olds into 83 regions of interest. *Neuroimage*. 2008;40:672-684.
4. Faillenot I, Heckemann RA, Frot M, Hammers A. Macroanatomy and 3D probabilistic atlas of the human insula. *Neuroimage*. 2017;150:88-98.
5. Thomas BA, Cuplov V, Bousse A, et al. PETPVC: a toolbox for performing partial volume correction techniques in positron emission tomography. *Phys Med Biol*. 2016;61:7975-7993.

The Journal of NUCLEAR MEDICINE

Reshaping the amyloid buildup curve in Alzheimer's disease? – Partial volume effect correction of longitudinal amyloid PET data

Michael Rullmann, Anke McLeod, Michel Grothe, Osama Sabri and Henryk Barthel

This article and updated information are available at:
http://jnm.snmjournals.org/content/early/2020/04/30/jnumed.119.238477

Information about reproducing figures, tables, or other portions of this article can be found online at:
http://jnm.snmjournals.org/site/misc/permission.xhtml

Information about subscriptions to JNM can be found at:
http://jnm.snmjournals.org/site/subscriptions/online.xhtml

JNM ahead of print articles have been peer reviewed and accepted for publication in *JNM*. They have not been copyedited, nor have they appeared in a print or online issue of the journal. Once the accepted manuscripts appear in the *JNM* ahead of print area, they will be prepared for print and online publication, which includes copyediting, typesetting, proofreading, and author review. This process may lead to differences between the accepted version of the manuscript and the final, published version.

SNMMI | SOCIETY OF NUCLEAR MEDICINE AND MOLECULAR IMAGING